Extraordinary Indentation Strain Stiffening Produces Superhard Tungsten Nitrides

Cheng Lu, Quan Li, Yanming Ma, and Changfeng Chen

Phys. Rev. Lett. **119**, 115503 — Published 15 September 2017

DOI: 10.1103/PhysRevLett.119.115503

Extraordinary Indentation Strain Stiffening Produces Superhard Tungsten Nitrides

Cheng Lu,[1] Quan Li,[2,3] Yanming Ma,[3] and Changfeng Chen[1]

[1]*Department of Physics and High Pressure Science and Engineering Center, University of Nevada, Las Vegas, Nevada 89154, USA*
[2]*College of Materials Science and Engineering, Jilin University, Changchun 130012, China*
[3]*State Key Laboratory of Superhard Materials, Jilin University, Changchun 130012, China*

(Dated: May 22, 2017)

Transition-metal light-element compounds are a class of designer materials tailored to be a new generation of superhard solids, but indentation strain softening has hitherto limited their intrinsic load-invariant hardness to well below the 40 GPa threshold commonly set for superhard materials. Here we report findings from first-principles calculations that two tungsten nitrides, hP4-WN and hP6-WN_2, exhibit extraordinary strain stiffening that produces remarkably enhanced indentation strengths exceeding 40 GPa, raising exciting prospects of realizing the long-sought nontraditional superhard solids. Calculations show that hP4-WN is metallic both at equilibrium and under indentation, marking it as the first known intrinsic superhard metal. An x-ray diffraction pattern analysis indicates the presence of hP4-WN in a recently synthesized specimen. We elucidate the intricate bonding and stress response mechanisms for the identified structural strengthening, and the insights may help advance rational design and discovery of additional novel superhard materials.

PACS numbers: 61.50.-f, 62.20.-x, 71.20.-b, 81.40.Jj

Traditional superhard materials like diamond and cubic boron nitride are indispensable to fundamental study and practical application in many fields of science and technology [1]. These strong covalent solids require stringent high pressure and high temperature synthesis and sintering conditions; moreover, diamond oxidizes in air and reacts with ferrous metals at moderate temperatures. Such constraints impose limits on practicality and applicability of these materials. Recently a rational design strategy has been pursued [2–11] to tailor a new generation of superhard materials by combining light elements (LEs) like boron and nitrogen with heavy transition metals (TMs), and it is expected that TM atoms would contribute high valence electron density to enhance incompressibility and LE atoms would form strong covalent network to strengthen the crystal structure.

Among TM-LE compounds TM borides have attracted considerable interest in recent years because of their favorable synthesis conditions and promising mechanical properties [9, 10, 12–17]. There have been reports of TM borides with hardness up to 50-60 GPa [18, 19]; however, these large hardness values are obtained only at very small loading forces or estimated using properties at the equilibrium structure, and results measured at large indentation loading drop by as much as 60-80% [20, 21]. Such load-dependent hardness readings do not offer an accurate measure of the indented material's ability to resist large plastic deformation; the material's intrinsic hardness is commonly defined by the load-independent value reached at large indentation loadings [22, 23]. All TM-LE compounds reported to date exhibit intrinsic load-independent hardness in the 15-30 GPa range, well below the 40 GPa threshold for superhard materials; first-principles calculations reveal large indentation strain softening as the main cause for the unexpectedly low load-invariant hardness [24–29]. Indentation strain stiffening, which is uncommon among crystalline solids, can greatly enhance indentation hardness as recently seen in some traditional superhard materials [30–33]. This mechanism may hold the key to producing the long-sought intrinsic superhard TM-LE compounds. Recent report of high-pressure synthesis of tungsten nitrides [34] has stimulated great interest in searching for such compounds in a new series of TM nitrides.

In this Letter, we present compelling findings of extraordinary indentation strain stiffening in two tungsten nitrides, hP4-WN and hP6-WN_2, which produces remarkably enhanced indentation strengths above 40 GPa. First-principles calculations show that hP4-WN is metallic both at equilibrium and under large indentation, while hP6-WN_2 undergoes a semiconductor-to-metal transition accompanying the indentation strengthening. Our results designate these tungsten nitrides as the first intrinsic superhard materials outside the family of traditional strong covalent solids and, in particular, place hP4-WN as the first intrinsic superhard metal. Energetic and lattice dynamic data indicate that both compounds are at least metastable; a structural analysis indicates the presence of hP4-WN in synthesized W-N specimen. A study of indentation induced structural evolution unveils delicate bonding changes underlying the remarkable structural strengthening. These insights elucidate fundamental mechanisms for superior indentation strengths of these outstanding tungsten nitrides and pave the way for rational design and discovery of more TM-LE compounds as a new generation of superhard solids.

Stress-strain relations from first-principles calculations can accurately describe material deformation and strength under diverse loading conditions [35–45], and calculated indentation strengths can be directly com-

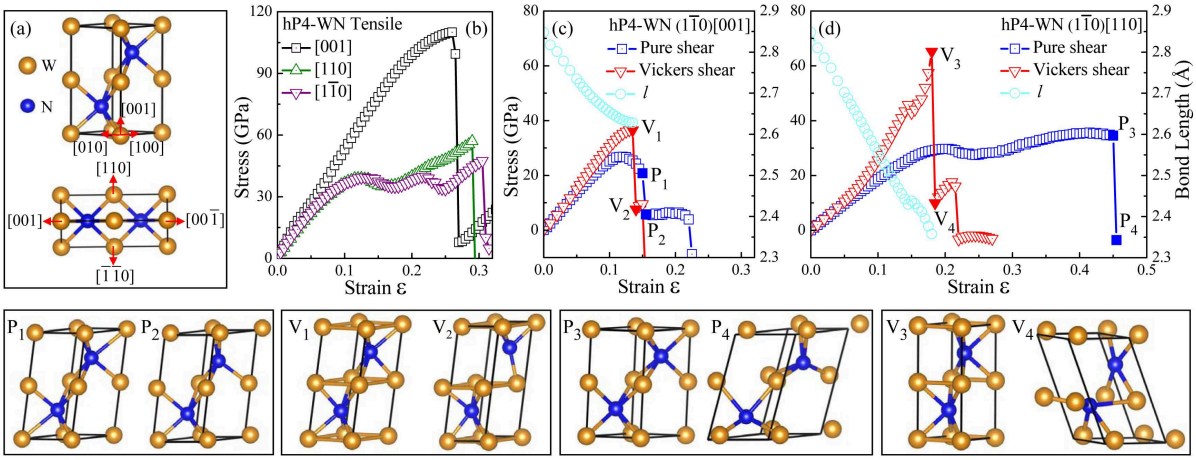

FIG. 1: (a) The crystal structure of hP4-WN at equilibrium (top) and projected onto the (1$\bar{1}$0) plane (bottom); (b) calculated stress responses under tensile strains along various high-symmetry directions; (c,d) calculated stress responses under pure shear and indentation shear strains in the (1$\bar{1}$0) plane along the [001] or [110] shear direction, and the W-W bond length (l) in the (001) plane up to the peak indentation strain. The bottom panels show the structural snapshots at two key points before and after the large drop of stress on each stress-strain curve under pure and indentation strains shown in (c) and (d).

pared to well-controlled nanoindentation measurements [46–48]. Under indentation, shear instability usually precedes the initiation of cracks and dislocations [49], signaling the onset of incipient plasticity [38, 40], and bond collapse may also occur under a compressive stress [50, 51]. Determination of indentation strength is achieved by calculations under a biaxial stress field that contains a shear (σ_{zx}) and a normal compressive (σ_{zz}) stress component that obey the relation $\sigma_{zz} = \sigma_{zx} tan\phi$, where ϕ is the centerline-to-face angle of the indenter [50, 51]. We have performed calculations for many TM-LE compounds, especially TM borides, and the obtained indentation strengths describe well the measured load-invariant indentation hardness [24–29]. We adopted this method to assess tungsten nitrides in the present work.

Recent studies using the latest crystal structure search techniques have identified a number of stable and metastable W-N phases [52, 53]. We have calculated stress-strain relations of all the stable and some metastable W-N phases in search of intrinsic superhard structures [54], and this systematic screening has led to the finding of two tungsten nitrides, hP4-WN and hP6-WN_2, that exhibit large indentation strength exceeding 40 GPa. We focus our discussion in this work on these two superhard phases, leaving a detailed analysis of all other studied W-N structures to a followup work.

Tensile stresses along high-symmetry directions are first examined to find the weakest tensile directions that determine the easy cleavage planes [35, 44], and indentation shear stresses in these planes are then obtained to assess indentation strengths [50, 51]. The structure of hP4-WN [Fig. 1(a)] belongs to space group $P6_3/mmc$ and has the lattice parameters a=2.848 Å and c=5.790 Å with the W and N atoms occupying the Wyckoff positions of 2a (0.0000, 0.0000, 0.0000) and 2c (0.3333, 0.6667, 0.2500), respectively. Its tensile stress along the [1$\bar{1}$0] direction has the lowest peak value, making (1$\bar{1}$0) the dominant easy cleavage plane. Our calculations have identified significant indentation strain stiffening in this plane along two inequivalent shear directions, (1$\bar{1}$0)[001] and (1$\bar{1}$0)[110]. Results in Fig. 1(c) and 1(d) show an enhancement of indentation strength from 26.8 GPa to 36.5 GPa, a 36% increase, under the (1$\bar{1}$0)[001] Vickers shear and from 35.7 GPa to 65.2 GPa, a remarkable 83% enhancement, under the (1$\bar{1}$0)[110] Vickers shear. Since these two shear directions are each two-fold symmetric and perpendicular to each other [see Fig. 1(a)], an indentation test that pushes against both directions is expected to produce indentation strength and the corresponding hardness exceeding 40 GPa, making hP4-WN the first intrinsic superhard material outside the family of traditional all-light-element superhard solids. Remarkably, calculations (see Fig. S1 in Supplemental Material (SM) [61]) indicate that hP4-WN is metallic both at equilibrium and under indentation, placing this material as the first known intrinsic superhard metal. It is noted that in synthesized specimens the calculated stress-strain curves may not always be followed, potentially leading to somewhat lower peak strength values.

To understand the extraordinary indentation strain stiffening in hP4-WN, which is unprecedented among TM-LE compounds, it is instructive to examine atomic deformation modes of the indented crystal lattice in comparison with that under pure shear deformation. In both cases shown in Fig. 1 (c) and 1(d), the stress response under indentation shear is nearly identical to that under pure shear at small strains, but further indentation causes greatly enhanced stiffness. The major contri-

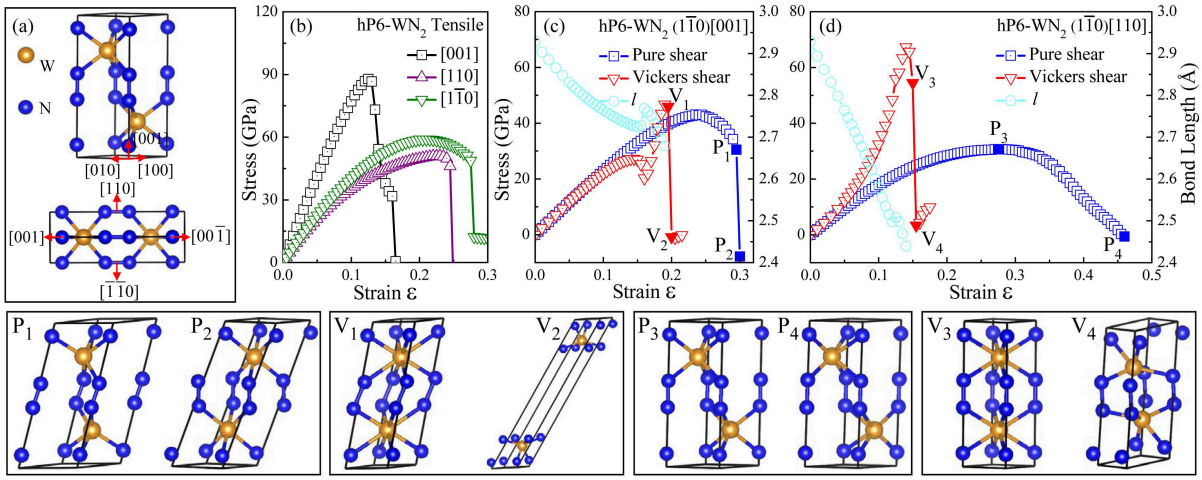

FIG. 2: (a) The crystal structure of hP6-WN_2 at equilibrium (top) and projected onto the (1$\bar{1}$0) plane (bottom); (b) calculated stress responses under tensile strains along various high-symmetry directions; (c,d) calculated stress responses under pure shear and indentation shear strains in the (1$\bar{1}$0) plane along the [001] or [110] shear direction, and the W-W bond length (l) in the (001) plane up to the peak indentation strain. The bottom panels show the structural snapshots at two key points before and after the large drop of stress on each stress-strain curve under pure and indentation strains shown in (c) and (d).

bution to this indentation strain stiffening stems from the shortening, thus strengthening of the W-W metallic bonds in the (001) planes, which is driven by the normal compression (σ_{zz}) that is absent under pure shear strains. The corresponding W-W bond length decreases from 2.848 Å at equilibrium to 2.628 Å at the peak-stress strain of 0.135 under the (1$\bar{1}$0)[001] indentation shear [see Fig. 1(c)]. This shortened W-W bond length is well below the typical W-W metallic single bond (2.756 Å) in α-W [62]. These W-W bonds, which become appreciably stronger as the compression increases, considerably strengthen the base of the trigonal prism units in the crystal structure, as seen in the structural snapshot V_1 taken at the peak strength shown in Fig. 1, and the resulting strong three-dimensional trigonal-prism network significantly enhances the structure's ability to resist deformation, whereas in the pure shear case, the prism base comprises much longer and weaker W-W bonds that slightly increase at increasing strains up to the breaking of a key W-N bond leading to a sharp drop of stress, as seen in snapshots P_1 and P_2 shown in Fig. 1. Under the (1$\bar{1}$0)[110] indentation shear, the situation is similar; but the strain stiffening is even more pronounced. This result is attributed to a more dramatic shortening (to 2.430 Å) of the W-W bonds in the (001) plane when sheared in the [110] direction, which, in turn, further strengthens the crystal structure against the indentation shear deformation. Another key factor in making and holding the tightly bound trigonal-prism network during the indentation process is the strong bonding between the nitrogen and tungsten atoms; the W-N bond lengths increase only a few percentage points from equilibrium to the peak-stress strains, resulting in an overall reduction in the volume of the hP4-WN structure. This strong W-N bonding prevents a large lateral lattice expansion under the Vickers indentation loading, which is the main mechanism for the indentation softening observed in other TM-LE compounds [24–29].

The hP6-WN_2 structure [see Fig. 2(a)] also belongs to space group $P6_3/mmc$ and has the lattice parameters a=2.928 Å and c=7.789 Å with the W and N atoms occupying the Wyckoff positions of 2d (0.3333, 0.6667, 0.7500) and 4e (0.0000, 0.0000, 0.5901), respectively. Calculated peak tensile stresses along the [110] and [1$\bar{1}$0] directions [Fig. 2(b)] are very close, making them both viable cleavage planes. Here we focus on the (1$\bar{1}$0) plane that manifests intrinsic superhard behavior driven by indentation strain stiffening. Under the (1$\bar{1}$0)[001] pure shear hP6-WN_2 exhibits a high peak stress of 43.0 GPa [Fig. 2(c)], but the peak stress under the (1$\bar{1}$0)[110] pure shear is much lower at 30.7 GPa. Indentation strains induce a semiconductor-to-metal transition (Fig. S2 in SM [61]) and strength enhancement. Under the (1$\bar{1}$0)[001] Vickers indentation, the stress response is similar to that under the pure shear strains, but the stress then dips slightly followed by a sharp rise to a peak stress of 46.7 GPa, an enhancement over the pure shear strength of 43.0 GPa. An examination of the bonding change during the deformation process reveals that the dip stems from a bond rotation mode (Fig. S3 in SM [61]) similar to that under pure shear deformation (see snapshots P_1 and P_2 in Fig. 2); upon further loading the normal indentation stress (σ_{zz}) compresses the atomic layers in the [1$\bar{1}$0] direction and promotes additional bonding between the W atom with the surrounding N atoms, resulting in an eight-coordinated W-N bonding configuration in contrast

to the six-coordinated one at equilibrium. Moreover, key W-N and W-W bond lengths are reduced by compression similar to the situation in hP4-WN. Consequently, the N-N bonds become the most strained load bearing units, producing the sharp rise of stress until the breaking of the N-N bonds [see snapshots V_1 and V_2 in Fig. 2]. Under the $(1\bar{1}0)[110]$ indentation shear, a robust stress response is produced by the compression induced bond strengthening accompanied by a similar transition from six-coordinated to eight-coordinated W-N bonding configuration with the peak stress reaching 67.4 GPa; here the main load bearing units are the eight-coordinated W-N bonds, and the breaking of three such W-N bonds marks the peak indentation shear strength [see Fig. 2(d) and snapshots V_3 and V_4].

Our study indicates that stress response is sensitive to the crystallographic planes chosen for indentation loading. For hP4-WN and hP6-WN_2 the indentation strain stiffening occurs in dominant or viable easy cleavage planes, making it relatively easy to realize, although care needs to be taken in preparing the cleavage surfaces. Our phonon calculations also show that these two tungsten nitride structures remain dynamically stable up to their respective peak indentation shear strains (see Fig. S6 in SM [61]). The strength values also depend on exchange correlation functionals used in calculations. We have performed calculations for hP4-WN and hP6-WN_2 in the $(1\bar{1}0)$ plane using the local density approximation (LDA), and the obtained indentation shear strengths (Fig. S4 in SM [61]) are higher than the generalized gradient approximation (GGA) results shown above. Actual values are expected to lie between the LDA and GGA results, firmly placing the two tungsten nitrides in the superhard category.

We now comment on possible synthesis of the tungsten nitrides studied here. Recent experiments [34] reported on four batches of specimens; among these the two synthesized and sintered at higher pressure and temperature conditions possess better crystallinity and deserve close attention. Based on a simple fitting scheme, the two structures were designated as cP7-W_3N_4 (space group $Pm\bar{3}m$) and hP2-WN (space group $P\bar{6}2m$), respectively. However, both structures show extensive imaginary phonon modes (Fig. S5 in SM [61]) and are therefore dynamically unstable. In this work, we have performed extensive refitting of the measured x-ray diffraction (XRD) spectra using the stable and some metastable structures from the latest structure search work [52]. The results show that the experimental XRD previously assigned as cP7-W_3N_4 is fit perfectly by the cubic cP6-WN phase [see Fig. 3(a)], which has been identified as a stable phase [52]. Phonon calculations show that cP6-WN along with hP4-WN and hP6-WN_2 are all dynamically stable (Fig. S5 in SM [61]). Meanwhile, the previously poorly fit and puzzling XRD for the experimentally assigned hP2-WN phase is well fit [Fig. 3(b)] by the hP4-

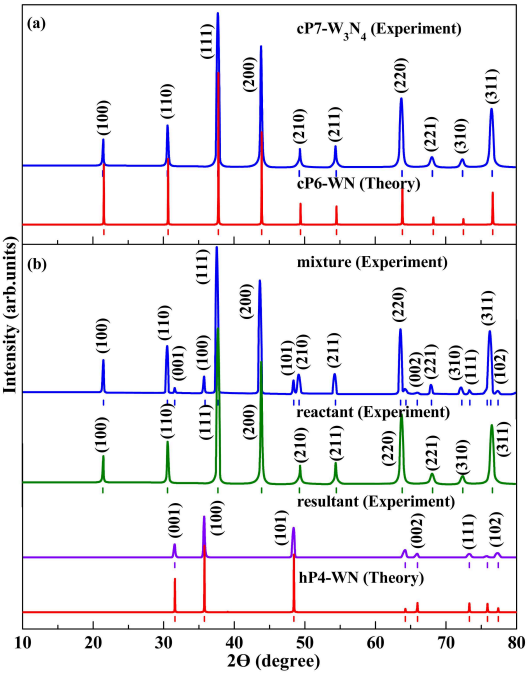

FIG. 3: (a) Fitting experimental XRD on a synthesized tungsten nitride specimen [34] by the cP6-WN phase. (b) Fitting experimental XRD on another tungsten nitride specimen by separating the measured spectra into two sets, one from the reactant cP6-WN phase and the other from the resultant hP4-WN phase. The x-ray wavelength is λ_{Cu}=1.5406 Å.

WN phase after the subtraction of the XRD spectra of the cP6-WN phase, which was used as the starting reactant material for preparing the fourth batch of specimen in the reported experiment [34]. This result suggests that the sintering at high pressure and temperature induced a partial transformation from cP6-WN to hP4-WN, and it points to a possible way to produce pure hP4-WN phase. While there has been no report on the synthesis of hP6-WN_2, a thermodynamic stability analysis has predicted [52] that this phase is viable for synthesis.

In summary, we have identified by first-principles calculations two tungsten nitrides, hP4-WN and hP6-WN_2, as intrinsic superhard materials with load invariant indentation strength exceeding 40 GPa. These are the first non-traditional superhard materials outside the family of all-light-element strong covalent solids; furthermore, hP4-WN is predicted to be the first known superhard metal, making it uniquely qualified for applications where superhardness and electric conduction are both desired. The extraordinary indentation strain stiffening in these tungsten nitrides stems from the indentation compression induced strengthening and coordination number increase of the W-N bonds and a significant contribution from the compression shortened and strengthened W-W metallic bonds. The superhard behavior is also sensitive to the crystal structure and the orientation of the in-

dented cleavage plane. These insights offer key guidance for seeking additional superhard materials in the large family of TM-LE compounds, especially transition-metal nitrides crystalized in hexagonal structures.

This work was supported in part by DOE under Cooperative Agreement DE-NA0001982 at UNLV and NSFC (Nos. 11622432, 11474125, and 11274136) at JLU.

[1] V. V. Brazhkin, A. G. Lyapin, and R. J. Hemley, Philos. Mag. A **82**, 231 (2002).

[2] E. Gregoryanz, C. Sanloup, M. Somayazulu, J. Badro, G. Fiquet, H. Mao, and R. J. Hemley, Nat. Mater. **3**, 294 (2004).

[3] R. B. Kaner, J. J. Gilman, and S. H. Tolbert, Science **308**, 1268 (2005).

[4] R. W. Cumberland, M. B. Weinberger, J. J. Gilman, S. M. Clark, S. H. Tolbert, and R. B. Kaner, J. Am. Chem. Soc. **127**, 7264 (2005).

[5] J. C. Crowhurst, A. F. Goncharov, B. Sadigh, C. L. Evans, P. G. Morrall, J. L. Ferreira, and A. J. Nelson, Science **311**, 1275 (2006).

[6] A. F. Young, C. Sanloup, E. Gregoryanz, S. Scandolo, R. J. Hemley, and H. Mao, Phys. Rev. Lett. **96**, 155501 (2006).

[7] H. Y. Chung, M. B. Weinberger, J. B. Levine, A. Kavner, J. M. Yang, S. H. Tolbert, and R. B. Kaner, Science **316**, 436 (2007).

[8] J. B. Levine, S. L. Nguyen, H. I. Rasool, J. A. Wright, S. E. Brown, and R. B. Kaner, J. Am. Chem. Soc. **130**, 16953 (2008).

[9] Q. Gu, G. Krauss, and W. Steurer, Adv. Mater. **20**, 3620 (2008).

[10] J. Q. Qin, D. W. He, J. H. Wang, L. M. Fang, L. Lei, Y. J. Li, J. Hu, Z. L. Kou, and Y. Bi, Adv. Mater. **20**, 4780 (2008).

[11] A. Friedrich, B. Winkler, L. Bayarjargal, W. Morgenroth, E. A. Juarez-Arellano, V. Milman, K. Refson, M. Kunz, and K. Chen, Phys. Rev. Lett. **105**, 085504 (2010).

[12] R. Mohammadi, A. T. Lech, M. Xie, B. E. Weaver, M. T. Yeung, S. H. Tolbert, and R. B. Kaner, Proc. Natl. Acad. Sci. USA **108**, 10958 (2011).

[13] M. Xie, R. Mohammadi, Z. Mao, M. M. Armentrout, A. Kavner, R. B. Kaner, and S. H. Tolbert, Phys. Rev. B **85**, 064118 (2012).

[14] X. Cheng, W. Zhang, X. Chen, H. Niu, P. Liu, K. Du, G. Liu, D. Li, H. Cheng, H. Ye, and Y Li, Appl. Phys. Lett. **103**, 171903 (2013).

[15] M. Wang, Y. Li, T. Cui, Y. Ma, and G. Zou, Appl. Phys. Lett. **93**, 101905 (2008).

[16] Q. Tao, D. Zheng, X. Zhao, Y. Chen, Q. Li, Q. Li, C. Wang, T. Cui, Y. Ma, X. Wang, and P. Zhu, Chem. Mater. **26**, 5297 (2014).

[17] M. Xie, R. Mohammadi, C. L. Turner, R. B. Kaner, A. Kavner, and S. H. Tolbert, Phys. Rev. B **90**, 104104 (2014).

[18] H. Niu, J. Wang, X. Q. Chen, D. Li, Y. Li, P. Lazar, R. Podloucky, and A. N. Kolmogorov, Phys. Rev. B **85**, 144116 (2012).

[19] H. Gou, N. Dubrovinskaia, E. Bykova, A. A. Tsirlin, D. Kasinathan, W. Schnelle, A. Richter, M. Merlini, M. Hanfland, A. M. Abakumov, D. Batuk, G. Van Tendeloo, Y. Nakajima, A. N. Kolmogorov, and L. Dubrovinsky, Phys. Rev. Lett. **111**, 157002 (2013).

[20] A. Knappschneider, C. Litterscheid, D. Dzivenko, J. A. Kurzman, R. Seshadri, N. Wagner, J. Beck, R. Riedel, and B. Albert, Inorg. Chem. **52**, 540 (2013).

[21] Q. Wang, J. He, W. Hu, Z. Zhao, C. Zhang, K. Luo, Y. Lü, C. Hao, W. Lü, Z. Liu, D. Yu, Y. Tian, and B. Xu, J. Materiomics **1**, 45 (2015).

[22] C. A. Brookes and E. J. Brookes, Diamond Relat. Mater. **1**, 13 (1991).

[23] H. Sumiya and T. Irifune, Diamond Relat. Mater. **13**, 1771 (2004).

[24] C. Zang, H. Sun, and C. F. Chen, Phys. Rev. B **86**, 180101(R) (2012).

[25] C. Zang, H. Sun, J. S. Tse, and C. F. Chen, Phys. Rev. B **86**, 014108 (2012).

[26] B. Li, H. Sun, C. Zang, and C. F. Chen, Phys. Rev. B **87**, 174106 (2013).

[27] B. Li, H. Sun, and C. F. Chen, Phys. Rev. B **90**, 014106 (2014).

[28] H. Wu, H. Sun and C. F. Chen, Appl. Phys. Lett. **105**, 211901 (2014).

[29] Q. Li, D. Zhou, W. Zheng, Y. Ma, and C. F. Chen, Phys. Rev. Lett. **115**, 185502 (2015).

[30] Y. Tian, B. Xu, D. Yu, Y. Ma, Y. Wang, Y. Jiang, W. Hu, C. Tang, Y. Gao, K. Luo, Z. Zhao, L. M. Wang, B. Wen, J. He, and Z. Liu, Nature **493**, 385 (2013).

[31] Q. Huang, D. Yu, B. Xu, W. Hu, Y. Ma, Y. Wang, Z. Zhao, B. Wen, J. He, Z. Liu, and Y. Tian, Nature **510**, 250 (2014).

[32] B. Li, H. Sun, and C. F. Chen, Nat. Commun. **5**, 4965 (2014).

[33] B. Li, H. Sun, and C. F. Chen, Phys. Rev. Lett. **117**, 116103 (2016).

[34] S. Wang, X. Yu, Z. Lin, R. Zhang, D. He, J. Qin, J. Zhu, J. Han, L. Wang, H. K. Mao, J. Zhang, and Y. Zhao, Chem. Mater. **24**, 3023 (2012).

[35] R. H. Telling, C. J. Pickard, M. C. Payne, and J. E. Field, Phys. Rev. Lett. **84**, 5160 (2000).

[36] H. Chacham and L. Kleinman, Phys. Rev. Lett. **85**, 4904 (2000).

[37] S. H. Jhi, S. G. Louie, M. L. Cohen, and J. W. Morris, Jr., Phys. Rev. Lett. **87**, 075503 (2001).

[38] S. Ogata, J. Li, and S. Yip, Science **298**, 807 (2002).

[39] D. M. Clatterbuck, C. R. Krenn, M. L. Cohen, and J. W. Morris, Jr., Phys. Rev. Lett. **91**, 135501 (2003).

[40] S. Ogata, J. Li, N. Hirosaki, Y. Shibutani, and S. Yip, Phys. Rev. B **70**, 104104 (2004).

[41] X. Blase, P. Gillet, A. San Miguel, and P. Mélinon, Phys. Rev. Lett. **92**, 215505 (2004).

[42] Y. Zhang, H. Sun, and C. F. Chen, Phys. Rev. lett. **93**, 195504 (2004).

[43] Y. Zhang, H. Sun, and C. F. Chen, Phys. Rev. Lett. **94**, 145505 (2005).

[44] Y. Zhang, H. Sun, and C. F. Chen, Phys. Rev. B **73**, 144115 (2006).

[45] M. G. Fyta, I. N. Remediakis, P. C. Kelires, and D. A. Papaconstantopoulos, Phys. Rev. Lett. **96**, 185503 (2006).

[46] C. R. Krenn, D. Roundy, Marvin L. Cohen, D. C. Chrzan, and J. W. Morris, Jr., Phys. Rev. B **65**, 134111 (2002).

[47] M. I. Eremets, I. A. Trojan, P. Gwaze, J. Huth, R. Boehler, and V. D. Blank, Appl. Phys. Lett. **87**, 141902

(2005).
[48] T. Li, J. W. Morris, Jr., N. Nagasako, S. Kuramoto, and D. C. Chrzan, Phys. Rev. Lett. **98**, 105503 (2007).
[49] A. Gouldstone, H. J. Koh, K. Y. Zeng, A. E. Giannakopoulos, and S. Suresh, Acta. Mater. **48**, 2277 (2000).
[50] Z. C. Pan, H. Sun, and C. F. Chen, Phys. Rev. Lett. **98**, 135505 (2007).
[51] Z. C. Pan, H. Sun, and C. F. Chen, Phys. Rev. Lett. **102**, 055503 (2009).
[52] M. J. Mehl, D. Finkenstadt, C. Dane, G. L. W. Hart, and S. Curtarolo, Phys. Rev. B **91**, 184110 (2015).
[53] Z. Zhao, K. Bao, D. Duan, F. Tian, Y. Huang, H. Yu, Y. Liu, B. Liu, and T. Cui, Phys. Chem. Chem. Phys. **17**, 13397 (2015).
[54] We have performed calculations using the Vienna Ab Initio Simulation Package (VASP) code [55], adopting two sets of density functionals, namely the local density approximation (LDA) with the exchange-correlation functional of Ceperley and Alder [56] as parametrized by Perdew and Zunger [57], and the Perdew-Burke-Ernzerh generalized gradient approximation (GGA) [58]. The electron-ion interaction was described by the projector augmented wave (PAW) approach [59] with $5d^4 6s^2$ and $2s^2 2p^3$ electrons as valence for W and N atoms, respectively. A cutoff energy of 700 eV for the expansion of the wave function into plane waves and sufficiently fine Monkhorst-Pack k-point sampling meshes [60] were chosen to ensure that all the enthalpy calculations are converged to better than 1 meV/atom. The shape of the unit cell is determined by the full atomic relaxation without any imposed boundary conditions with the stress convergence set to 0.1 GPa.
[55] G. Kresse and J. Furthmller, Phys. Rev. B, **54**, 11169 (1996).
[56] D. M. Ceperley and B. J. Alder, Phys. Rev. Lett. **45**, 566 (1980).
[57] J. P. Perdew and A. Zunger, Phys. Rev. B **23**, 5048 (1992).
[58] J. P. Perdew, K. Burke, and M. Ernzerhof, Phys. Rev. Lett. **77**, 3865 (1996).
[59] G. Kresse and D. Joubert, Phys. Rev. B **59**, 1758 (1999).
[60] H. J. Monkhorst and J. D. Pack, Phys. Rev. B, **13**, 5188 (1976).
[61] Supplemental material on calculated electronic density of states for hP4-WN and hP6-WN_2 at equilibrium and indented structures, a deformation mode of hP6-WN_2 under indentation, indentation strengths of hP4-WN and hP6-WN_2 calculated under LDA, and calculated phonon dispersion for various W-N compounds.
[62] L. Pauling and B. Kamb, Proc. Natl. Acad. Sci. USA **83**, 3569 (1986).